Kremen1 dependence receptor induces SEC24C- and ATG9A-dependent autophagic cell death

Sonia Brahim[1,2,*], Thomas Schott[2*], Shiva Ghasemi[1*], Ana Negulescu[2], Clara Geneste[2], Elisabeth Errazuriz-Cerda[3], Gabriel Ichim[1], Patrick Mehlen[1] and Olivier Meurette[1,2,$]

[1]Cancer Cell Death Laboratory, LabEx DEVweCAN, Centre de Recherche en Cancérologie de Lyon, INSERM U1052-CNRS UMR5286, Université de Lyon, Centre Léon Bérard, 69008 Lyon, France.

[2]Apoptosis, Cancer and Development Laboratory- Equipe labellisée 'La Ligue', LabEx DEVweCAN, Centre de Recherche en Cancérologie de Lyon, INSERM U1052-CNRS UMR5286, Université de Lyon, Centre Léon Bérard, 69008 Lyon, France.

[3]Centre de l'Imagerie Quantitative Lyon Est, Faculté de Médecine Laënnec, Lyon, France.

[*]Co first authors

Corresponding author: O. Meurette; email: olivier.meurette@lyon.unicancer.fr.

ABSTRACT

Dependence receptors (DRs) induce cell death by apoptosis in the absence of their ligand. Among them, Kremen1 was first described to induce cancer cell death in the absence of its ligand, DKK1. Nevertheless, the exact mechanism of Kremen1-triggered cell death remains unexplored. In this study, we demonstrate that Kremen1 induces cell death with autophagic features, contrasting with the apoptotic process typically associated with dependence receptors. Specifically, chemical inhibition of autophagy by spautin or wortmannin or genetic inhibition of ATG9A or ATG18B effectively blocks this cell death process. Furthermore, through a proximity protein interactome analysis of Kremen1, we identified Sec24C, a component of the COP-II complex, as important effector of Kremen1-induced autophagy and cell death. Our findings reveal an interaction between Sec24C and ATG8 regulated by Kremen1, potentially underlying the increased number of autophagosomes in cancer cells, leading to their death. This correlation between Kremen1 and the induction of aberrant autophagy deserves particular attention, especially as the Kremen1/DKK1 pair is frequently altered in cancers, with higher DKK1 expression associated with poor survival outcomes. Thus, targeting this pathway may offer a potential strategy for treating cancers resistant to current therapies.

Keywords: Cancer, Cell death, ATG9A, SEC-24C, Dependence Receptors

44

45 **ABBREVIATIONS**

46

47 APEX: Ascorbate Peroxidase

48 ATG: Autophagy related genes

49 CNS: Central Nervous System

50 COP-II: Coat Protein Complex II

51 DKK1: Dickkopf-Wnt Signaling Pathway Inhibitor

52 DR: Dependence Receptor

53 LRP5/6: LDL Receptor Related Protein 5

54 PLA: Proximity Ligation assay

55 STING: Stimulator Of Interferon Response CGAMP Interactor

56 TCGA: The Cancer Genome Atlas

57 WNT: Wingless-related integration site

58

59

60

61

62

63

64

65

66

67 **INTRODUCTION**

68 Dependence receptors (DR) are a family of transmembrane receptor proteins crucial in
69 maintaining cellular homeostasis. Notably, they play a significant role in cancer progression by
70 regulating cell proliferation when bound to their ligand, and by inducing apoptosis in absence of
71 their ligand [1]. Despite their structural diversity, these receptors constitute a functional family, each
72 shown to induce apoptosis through different mechanisms [2–4]. Kremen1, a recently identified DR,
73 has been recognized for its ability to induce cell death in absence of its ligand, Dickkopf-Wnt
74 Signaling Pathway Inhibitor (DKK1) [5]. Initially characterized as a Wnt signaling inhibitor,
75 Kremen1/2 serves as a high-affinity receptor for DKK1. Together, they cooperate to recruit the
76 WNT co-receptor LRP5/6, thereby inhibiting the Wnt/β-catenin pathway [6]. Further studies
77 suggested that Kremen1/2 are not directly involved in this inhibition but they recruit DKK1 and
78 present it to LRP5/6 when the WNT coreceptor is in excess [7]. Once the ternary complex between
79 DKK1, Kremen1/2, and LRP5/6 is formed, it undergoes rapid clathrin-mediated endocytosis,
80 thereby limiting the number of available Wnt co-receptors on the plasma membrane [8,9]. Kremen1/2
81 has been implicated in essential developmental processes, including anteroposterior patterning of
82 the central nervous system (CNS) in *Xenopus* [10], as well as DKK1 in mice [11]. Kremen1 has also
83 more recently been described as a receptor for enteroviruses [12].

84 As observed with other DR, Kremen1/DKK1 receptor-ligand pair may play a significant
85 role in regulating cancer initiation and progression. Kremen1 expression is frequently lost in cell
86 lines derived from various cancers, including glioblastoma, neuroblastoma, lung cancer, kidney
87 cancer, stomach cancer, melanoma, and lymphoma [13]. Conversely, its ligand DKK1 is upregulated
88 in several primary tumor type and is elevated in the serum of cancer patients [14]. Furthermore, high
89 serum levels of DKK1 are associated with poor prognosis in breast, prostate and bladder cancers
90 [15–17], as its overexpression similarly correlated with poor outcomes in hepatocellular carcinoma [18].
91 As Kremen1 has been described as a DR inducing cell death independent from Wnt inhibition [5],
92 we thought to study how this DR induces cell death. Initial description of Kremen1-induced cell
93 death involved caspase-3 cleavage and subsequent activation. However, we mainly observed
94 autophagic features in dying cells that would never show apoptotic features but rather necrotic
95 swelling and plasma membrane permeabilization. Although caspases were slightly activated, their

inhibition was only associated to a minor rescue of cell death. The COP-II complex is emerging as an important regulator of autophagy induction with Sec24C as a key autophagy effector [19,20] in STING-associated autophagy and cell death [21,22]. Interestingly, we found that SEC24C is essential for Kremen1 and ATG8 to trigger autophagic cell death in an ATG9A-dependent manner. The signaling pathway triggered by Kremen1, especially in the context of tumorigenesis, remains poorly understood. Here, we demonstrate that, unlike other DRs, Kremen1 induces a form of cell death reliant on autophagy, rather than caspases and lacks traditional apoptotic features. Notably, Kremen1 expression is absent in various cancers, including breast carcinoma, where it serves as a favorable prognostic marker when DKK1 levels are low. Collectively, these findings suggest that Kremen1 acts as a tumor suppressor by inducing autophagy-dependent cell death in the absence of DKK1, indicating that the Kremen1/DKK1 pair may represent a promising therapeutic target in cancer.

RESULTS

Kremen1/DKK1 pair is altered in cancers

Given the established role of DR and their ligands in tumor suppression, we first examined the expression profiles of the Kremen1/DKK1 pair across various datasets. Consistent with characteristics of tumor suppressors, Kremen1 expression was reduced in multiple cancer types, including breast cancer (BRCA), colon cancer (COAD), and head and neck cancers (HNSCC) (Figure 1A). In contrast, DKK1 expression was markedly upregulated across several cancers (Figure 1B). Consistently, analysis of the The Cancer Genome Atlas (TCGA) dataset showed that patients with high DKK1 expression had worse overall survival in pancreatic ductal adenocarcinoma (PAAD) and in breast cancers (BRCA)(Figure 1C-D). Interestingly, DKK1 expression is higher in basal-like (TCGA data) and HER2-overexpressing breast cancers (Figure 1E), an observation corroborated in the METABRIC dataset, where DKK1 was elevated in HER2+ and HER2-/ER- subtypes (Figure 1F). In contrast, Kremen1 expression did not vary significantly by subtype in the TCGA dataset (Figure 1G), though it was slightly but significantly higher in HER2+ cases in the METABRIC dataset (Figure 1H). These findings suggest that alterations in the Kremen1/DKK1 pair may be particularly relevant in basal-like (ER-/HER2-) breast cancers, where DKK1 is highly expressed while Kremen1 is low. Consequently, we decided to focus on triple-negative breast cancers for further investigation. We also studied pancreatic cell lines given the predictive value of DKK1 in PDAC. Given Kremen1's role in Wnt inhibition in the presence of DKK1, we examined whether Wnt gene signatures were altered in patients with high Kremen1/DKK1 expression, but observed no significant differences meaning the expression of DKK1 and Kremen1 is not associated to Wnt signature (Supplementary figure 1A). Thus, the deregulated Kremen1/DKK1 expression ratio favoring DKK1 is a potential biomarker of poor prognosis.

138 **Kremen1 does not induce apoptotic cell death**

139 Kremen1 has previously been described as a DR inducing features of apoptotic cell death
140 [5]. In order to investigate the mechanisms underlying Kremen1-induced cell death, we developed
141 stable cell lines of triple-negative breast cancer MDA-MB-231 cells and of pancreatic cancer cell
142 line BxPC3 that express Kremen1 upon doxycycline induction. Cell death analysis using propidium
143 iodide staining demonstrated that doxycycline treatment induced cell death in both cell lines
144 (Figure 2A, supplementary figure 1B). Additionally, colony formation assays revealed a reduction
145 in colony formation upon Kremen1 induction (Figure 2B). Co-expression of DKK1 reduced
146 Kremen1-induced cell death, supporting the previously documented DR activity of Kremen1
147 (Figure 2C). Importantly, doxycycline treatment did not trigger cell death in control cells
148 (Supplementary figure 1B). Furthermore, the treatment of cells in the presence of siRNA targeting
149 DKK1 also induced cell death although to a lower extend than Kremen1 induction (Supplementary
150 Figure 2A). Kremen1 expression led to a dose-dependent activation of caspase-3, which was
151 efficiently inhibited by treatment with Q-VD- OPh pan-caspase inhibitor (Figure 2D). However,
152 treatment with Q-VD-OPh (QVD) inhibited only very partially cell death (Figure 2E). We also
153 treated cells with additional caspase inhibitors, including IETD and DEVD, and observed no
154 impact on cell death, indicating that these caspases are not involved in our cell death model
155 (Supplementary Figure 2C). Interestingly, treatment of Kremen1-expressing cells with ABT263
156 triggered a rapid shift towards apoptotic features, indicating that these cells remain responsive to
157 apoptotic stimuli and that Kremen1-induced caspase activity may prime cells to a stronger
158 apoptotic stimulus (Supplementary Figure 2D). Treatment of cells with BV6, used as an apoptotic
159 control to achieve the same level of cell death, revealed that caspase activation was weak in
160 Kremen1 treated cells compared to the control (Supplementary figure 2E). Furthermore, Kremen1-
161 expressing cells did not exhibit molecular markers of apoptosis, such as PARP-1 or caspase-3
162 cleavage, as shown by western blot analysis (Supplementary Figure 2F). Finally, Nanolive
163 microscope-based holotomography imaging of cells treated with doxycycline or BV6 as an
164 apoptotic inducer revealed distinct phenotypic differences in cell death. Cells treated with BV6
165 exhibited membrane blebbing and cell contraction, while Kremen1-overexpressing cells displayed
166 a phenotype characterized by cellular swelling and finally permeabilization of the plasma
167 membrane (Figure 2F). Thus, our results indicate that kremen1 induces a form of cell death distinct
168 from classical apoptosis.

169 **Kremen1 induced-cell death displays autophagic features**

170 Prior to examining the specific mechanisms of Kremen1-induced cell death, we analyzed
171 the morphology of dying cells using transmission electron microscopy (TEM). In fact, we did not
172 observe apoptotic features like membrane blebbing or nuclear condensation and cells appeared to
173 increase in volume rather than exhibit the typical apoptotic shrinkage (Figure 3A). Across multiple
174 time points, in both adherent and non-adherent cells, the dying cells consistently displayed
175 autophagic features, including an accumulation of vacuoles, phagophores, autophagosomes, and
176 multilamellar bodies (supplementary figure 3A). In the supernatant, rare apoptotic cells were
177 observed although most of dead cells appeared necrotic (Supplementary figure 3B). We confirmed
178 autophagy induction through molecular analyses, evidenced by the accumulation of the lipidated
179 form of LC3 and a decrease in p62 expression upon Kremen1 induction, as shown by western
180 blotting (Figure 3B), and the formation of dense LC3 puncta in immunofluorescence assays (Figure
181 3C,D) indicating that autophagosomes are increased in dying cells both in MDA-MB231 and
182 BxPC3 cells. Moreover, no LC3 lipidation was observed in control cells treated with doxycycline
183 (Supplementary figure 4A). In agreement with autophagy being regulated by the DR function of
184 Kremen1, cells re-expressing DKK1 induced a reduction in LC3B lipidation (supplementary figure
185 4B). Interestingly, p62 levels decreased transiently up to 24 hours and subsequently increased from
186 48h up to 72 hours (Supplementary figure 4C). This observation suggests that the autophagic flux
187 initially increases rapidly; however, at a certain point, it becomes blocked due to excessive
188 accumulation of autophagosomes, surpassing the cell's capacity. This imbalance may result in
189 impaired autophagic flux.

190 **The autophagic machinery is necessary for Kremen1-induced cell death.**

191 We next sought to assess the requirement of the autophagic machinery in the observed cell
192 death. Wortmannin as well a spautin treatment which inhibit the early stage of autophagic flux by
193 preventing autophagosome formation, resulted in a significant decrease in cell death and
194 autophagic flux (Figure 4 A,B). In contrast, treatment with Bafilomycin-A and Chloroquine, which
195 both block the flux at late stages inducing autophagosome accumulation led to an increase of cell
196 death following kremen1 expression (Figure 4 C,D). As expected, treatment with bafilomycine A1
197 and chloroquine induced further accumulation of lipidated form of LC3 and accumulation of p62
198 (supplementary figure 4D). This suggests that the presence of autophagosomes or certain

199 autophagic components may be essential for cell death induction. While autophagy is often induced
200 following apoptosis as a mechanism thought to inhibit cell death, in our model, treatment with
201 Spautin1 completely blocked cell death by inhibiting LC3 lipidation (Figure 4B) without affecting
202 caspase activation (Supplementary figure 4E). Surprisingly, knock-down of ATG5 by siRNA or
203 by CRISPR knock-down had no impact on cell death induction nor on caspases activation
204 (Supplementary figure 4F) showing that atypical autophagy is likely involved in this process. As
205 ATG5 was not involved in Kremen1-induced cell death, we examined the role of ATG9A, since it
206 is a protein which facilitates membrane recruitment and autophagosome membrane expansion [23].
207 We observed partial co-localization between Kremen1 and ATG9A (Figure 4E, supplementary
208 Figure EG). We further showed that inhibition of ATG9 via siRNA (supplementary Figure 4G)
209 significantly reduced cell death in both MDA-MB-231 and BxPC3 cell lines, highlighting its
210 essential role in this process (Figure 4F). We also investigated the involvement of ATG18 and
211 ATG2 since they have shown to participate with ATG9A to autophagosome membrane expansion
212 [24]. siRNA mediated knock-down of ATG2 alone induced a high amount of cell death preventing
213 us to study its putative involvement in this context. In contrast ATG18B knock-down also rescued
214 Kremen1-induced cell death (Figure 4G). Altogether, these findings support the involvement of an
215 atypical form of autophagy relying on ATG9A and ATG18 to induce aberrant accumulation of
216 autophagosomes leading to autophagic cell death.

217 **SEC-24C is involved in Kremen1-induced cell death**
218
219 To elucidate the mechanisms underlying this autophagy-mediated cell death, we analyzed
220 the Kremen1 interactome via mass spectrometry. For this purpose, we employed a proximity
221 labeling approach by fusing Kremen1 with an ascorbate peroxidase (APEX2) enzyme to perform
222 enzyme-mediated biotin identification. Using the same doxycycline-inducible system, we
223 expressed a Kremen1-APEX fusion protein to identify proteins in close proximity. We first
224 confirmed that the Kremen1-APEX fusion did not alter K1-mediated signaling, as Kremen1-
225 APEX2 induced autophagy and cell death with comparable efficiency to Kremen1 alone (data not
226 shown). We then used streptavidin beads to isolate proteins proximal to Kremen1-APEX, followed
227 by mass spectrometry analysis, which yielded a list of proteins most enriched upon doxycycline
228 addition and subsequent Kremen1 induction (Figure 5A,B). Among the most enriched proteins
229 were SEC24C and other proteins of the COP-II complex. Two major clusters appeared using String-

230 database analysis (Figure 5B). The first one was enriched in membrane-associated, adhesion and
231 focal adhesion proteins such as integrins (ITGB1, ITGA6, ITGA2), taline (TLN1), vinculin (VCL),
232 paxillin (PXN), showing the membrane localization of Kremen1 in the experiments. The second
233 cluster was a cluster of COP-II complex proteins, including SEC23A and B, SEC24 B and C as
234 well as SEC31A. This complex particularly caught our attention since the COP-II complex has
235 been implicated in atypical autophagy regulation [19,20]. Specifically, SEC24C stands out due to its
236 role in autophagy regulation by its interaction with ATG9 to increase autophagosomes abundance
237 in yeast [25]. We first confirmed the Kremen1/SEC24C interaction through a proximity ligation assay
238 (PLA), observing that Kremen1 and SEC24C were indeed in close proximity (Figure 5C). This
239 interaction was also observed in BxPC3 cell line by confocal immunofluorescence (Figure 5D). To
240 investigate the potential role of SEC24C during Kremen1 cell death induction, we inhibited its
241 expression via siRNA and found a significant reduction of Kremen1-induced cell death in both
242 MDA-MB-231 and BxpC3 cell lines (Figure 5E).
243
244 **SEC24C is fostering autophagy induction by Kremen1**
245 We next looked at the role of SEC24C in Kremen1 induced autophagy. We observed that
246 SEC24C knock-down induced a reduction in autophagic markers following Kremen1 induction,
247 suggesting that SEC24C plays a crucial role in promoting autophagosome formation in response
248 to Kremen1 expression (Figure 6 A,B). We then sought to determine whether SEC24C was
249 associated with autophagosomes upon Kremen1-dependent cell death induction. To this end, we
250 performed immunoprecipitation of SEC24C in the presence and absence of Kremen1 and observed
251 that, upon Kremen1 induction, SEC24C interacted with ATG8, indicating that SEC24C plays a
252 specific role in autophagy regulation within this autophagic cell death pathway (Figure 6B). This
253 observation was further validated through confocal microscopy, which revealed the colocalization
254 of ATG8 and SEC24C in BxPC3 cells in condition of Kremen1 expression, as indicated by yellow
255 puncta (Figure 6C). Altogether, these findings demonstrate that SEC24C and the COP-II complex
256 are essential components in mediating Kremen1-induced cell death by increasing autophagy in
257 cells. Furthermore, DKK1 expression induced an inhibition of Kremen1 and ATG9A interaction,
258 as seen with PLA experiments (Figure 6D) showing that in absence of DKK1, Kremen1 interaction
259 with ATG9A vesicle is fostering autophagosome accumulation.
260

DISCUSSION

Kremen1, initially identified as a receptor involved in DKK1-mediated Wnt signaling inhibition [6], was later characterized as a DR [5]. DRs constitute a diverse family of structurally unrelated receptors that share the unique capacity to actively signal cell death in the absence of their respective ligands. Until now, all known DRs have been shown to induce apoptosis through distinct pathways that ultimately converge on caspase-3 activation [26]. In the case of Kremen1, Causeret et al. reported that its overexpression led to caspase-3 cleavage, consistent with an apoptotic pathway similar to that of other DRs. In this study, we confirmed that Kremen1 expression induces caspase-3 activation despite the absence of classical apoptotic features, as evidenced by transmission electron microscopy and Nanolive time-lapse microscopy. However, inhibition of caspase activity with qVD-Oph had no effect on cell death indicating that effector caspases are dispensable for Kremen-1 induced cell death. It is plausible to consider that caspase activation in this context occurs at a sub-lethal threshold, insufficient to directly induce cell death but potentially involved in non-apoptotic roles as it already has been shown before [27]. Another explanation would be that the aberrant increase of autophagosomes vacuoles may prevent the cleavage of canonical substrates necessary for apoptotic progression. However, cells expressing Kremen1 remain responsive to apoptotic stimuli, particularly in the early stages following Kremen1 induction, as treatment with ABT263, a Bcl-xL and Bcl-2 antagonist, rapidly induces canonical apoptosis indicating that cells remain sensitive to apoptotic stimuli.

Cells exhibiting autophagic features have long been reported in physiological cell death [28]. However, the presence of abundant autophagosomes in dying cells does not necessarily imply that autophagy is the direct trigger of cell death. Autophagy is well-established as a survival pathway under nutrient-limiting conditions [29] and it is generally considered to limit apoptosis and confer resistance to cell death [30]. Evidence from physiological development supports the role of autophagy as a *bona fide* cell death mechanism. In Drosophila, for example, autophagy, not apoptosis, is essential for programmed cell death in the midgut [31] and is also required for the degradation of salivary gland cells [32]. Additionally, autophagy-dependent cell death, termed autosis, can be induced by autophagy-stimulating peptides, such as Tat-Beclin1, which holds potential for therapeutic applications [33]. The cell death observed following Kremen1 induction displays phenotypic similarities with Tat-Beclin1-induced autosis. However, treatment with Na^+/K^+ inhibitors did not rescue this cell death (data not shown), suggesting mechanistic differences from

293 canonical autosis. Kremen1-induced cell death results in a substantial accumulation of
294 autophagosomes, which may contribute to the observed cytotoxicity. Autophagosome
295 accumulation alone has been reported as sufficient to induce cytotoxic effects [34] and the timing of
296 autophagosome accumulation relative to ATP availability and lysosomal homeostasis may be
297 critical factors [35]. Based on these studies, we hypothesize that Kremen1 induction triggers a
298 substantial increase in autophagy, resulting in elevated autophagosome formation that demands
299 extensive membrane resources and, consequently, significant ATP consumption. Through
300 proximity ligation assay and further immunoprecipitation and immunofluorescence analysis we
301 identified the COP-II complex as part of the Kremen1 interactome involved in autophagosomes
302 aberrant accumulation. The COP-II complex primarily serves two functions: it facilitates the
303 physical deformation of the endoplasmic reticulum membrane into vesicles and selects cargo
304 molecules for transport to the Golgi apparatus. Notably, SEC24C, a core component of this
305 complex, plays a significant role in autophagy. Under cellular stress, such as nutrient deprivation,
306 SEC24C undergoes phosphorylation by the kinase Hrr25, enabling it to interact with ATG9 [25]. This
307 interaction reroutes the COP-II complex towards the autophagic pathway, promoting an increase
308 in autophagosome formation. In line with this, SEC24C has also been implicated in ER-phagy [19]
309 and activation of the cGAS-STING pathway [21]. This is likely involved in Kremen1 induced cell
310 death although identification of putative SEC24C phosphorylation remains to be identified in this
311 context. However, both SEC24C and ATG9A are required for Kremen1-induced, autophagy-
312 dependent cell death. Beyond SEC24C, we identified additional SEC24 isoforms (A/B and D), as
313 well as SEC31 and SEC23, in the Kremen1 interactome via mass spectrometry. We also showed
314 that in presence of its ligands DKK1, Kremen1 is not or much less interacting with ATG9A. We
315 therefore hypothesize that upon Kremen1 induction or limitation for DKK1 ligand, Kremen1 is
316 recruiting ATG9A vesicle to SEC24C/ATG8 site of autophagosome formation creating an increased
317 demand for membrane resources to support autophagosome formation. Thus, genetic inhibition of
318 SEC24C of ATG9A prevents cell death by avoiding the massive accumulation of autophagosomes,
319 thereby reducing the associated metabolic stress from extensive autophagosome formation and the
320 high energy demands placed on lysosomal processing.

321 Given the relevance of DRs as therapeutic targets in cancer [26], we examined the status of
322 the Kremen1/DKK1 pair across various cancer types. Our observations indicate that Kremen1
323 expression is frequently downregulated in multiple cancers, suggesting a potential role for

Kremen1 as a tumor suppressor through its autophagy-dependent cell death pathway. Notably Sato et al [14] reported elevated DKK1 serum levels in patients, stronger than those observed here in RNA sequencing data. In breast cancer specifically, while some patients exhibited high DKK1 levels, the median expression of DKK1 in matched tumor/normal samples remained below 1 in breast tumors (Figure 1B), contrasting with the significant serum increases observed by Sato et al,. Additionally, DKK1 expression has been linked to metastasis and poor survival outcomes in lymph node-positive breast cancer patients [36]. Notably, recent studies have demonstrated that autophagic cell death may contribute to tumor suppression by limiting chromosomal instability [37,38]. We are currently exploring the therapeutic potential of activating this novel autophagic cell death pathway as a targeted approach in cancer treatment.

336 **EXPERIMENTAL PROCEDURES**

337 **Plasmids construction**

338 The inducible Sleeping Beauty transposon system was used as backbone for cloning the murin
339 Kremen1 gene under doxycycline inducible control. The Kremen1 gene was fused in N-terminal
340 with an HA tag. Two constructs were realized: pitr1-Kremen1, containing a GFP insertion
341 constitutively expressed and a puromycin resistant gene constitutively expressed and pitr2-
342 Kremen1 containing a RFP insertion and a zeocin resistant gene both constitutively expressed.

343 **Cell culture**

344 Human breast cancer cell line MDA-MB231 and human embryonic kidney HEK293T cells were
345 obtained from ATCC (UK) and maintained in Dulbecco's Modified Eagle's Medium (DMEM)
346 supplemented with 10% fetal bovine serum (FBS) and 1% penicillin/streptomycin.

347 For the establishment of stable cell lines MDA-MB231 and HEK293T with pitr1-Kremen1 or pitr2-
348 Kremen1, the cells were transfected with 1,6 µg plasmid, 0,4 µg SB100x transposase and Fugen
349 (Promega) in a ratio total DNA : transfectant of 1:3 and then selected with puromycin (Gibco Life
350 Technologies) or zeocin (Invitrogen) for 2 to 4 weeks. MDA-MB231 clones were selected by flow
351 cytometry in accordance with high or low expression of GFP.

352 For inhibitor treatments cells were incubated with 20 µM q-VD (Sigma-Aldrich SML0063), 40 µM
353 Necrostatin-1 (Sigma-Aldrich N9037), 5 mM 3-MethylAdenin (Sigma-Aldrich M9281) in
354 different combinations. For induction of Kremen1, Doxycycline (Sigma-Alderich) was added in
355 various concentrations in cell media.

356 siRNA transfections were realized in 6-well plates with 10nM siRNA and 3µl Lipofectamine
357 RNAiMAX (Life) according to the manufacturer instructions. The siRNA used were Life Silencer
358 Select Negative control #1 Cat#4390843, lot AS021N56;

359 **Transmission electron microscopy (TEM)**

360 Cells were prepared for fixation in 6-well plates or in surnatants with 1 volume complete DMEM
361 medium + 1 volume glutaraldehyde 4% for 15 minutes at 4°C. Cells were fixed in 1 volume

362 cacodylate pH 7,4 + 1volume g glutaraldehyde 4%. Attached cells were harvested by scratching
363 and centrifugated. The sample were washed three times in saccharose 0.4 M/0.2 M Na C-HCl-
364 Cacodylate-HCl pH 7.4 à 0,2 M for 1 hour at 4°C, and postfixed with 2% OsO4/0.3 M Na C-
365 HCl Cacodylate-HCl pH 7.4 1hour at 4°C. Then cells were dehydrated with a increading ethanol
366 gradient (5minutes in 30%, 50%, 70%, 95% and 3 times for 10 minutes in absolute ethanol.
367 Impregnation was performed with Epon A (50%) plus Epon B (50%) plus DMP30 (1,7%).
368 Inclusion was obtained by polymerisation at 60°C for 72hrs. Ultrathin sections (approximately 70
369 nm thick) were cut on a ultracut UC7 (Leica) ultramicrotome, mounted on 200 mesh copper grids
370 coated with 1:1000 polylisine, and stabilized for 1day at room temperature (RT) and, contrasted
371 with uranyl acetate and lead citrate. Sections were examinated with a Jeol 1400 JEM (Tokyo,Japan)
372 transmission electron microscope equipped with a Orius 600 camera and Digital Micrograph.

373 **Caspase-3 activity assay**

374 Cell were were harvest by trypsinization and cell pellets were obtained by centrifugation at 4°C
375 and lysed. The caspase-3 activity assay was performed according to the manufacturer's instructions
376 (Biovision caspase-3 colorimetric assay kit). Total protein concentrations were measured with the
377 BCA assay kit using BSA as a standard (Pierce Biotechnology, Rockford, IL, USA). Absorbance
378 readings were done on a TECAN infinite F500.

379 **PI/Sytoxgreen stained cells counting**

380 Cells were plated in 96-well plates, incubated with 0,33 ng/ml PI or Sytoxgreen and different
381 treatments. The plates were further monitored by Incucyte Zoom (Essenbio) for several days. The
382 PI positive cells were normalized by the confluence percentage for each well, at several time points.

383 **Immunofluorescence staining**

384 Fixation and staining were performed simultaneously. Attached cells samples were fixed with
385 freshly prepared 4% PFA , washed 3 times with PBS for 5 minutes and permeabilized with PBS-
386 0.2% Triton X-100 (TX-100) for 10 minutes at room temperature. Samples were then washed 3
387 times with PBS for 5 minutes and blocked in PBS with 4% bovine serum albumin (BSA), 2%
388 normal donkey serum and 0.2% TX-100 for one hour. Primary antibodies were diluted in the
389 blocking solution at a dilution of 1:200 for the anti-Kremen1 produced antibodies and 1:50 for anti-

390 HA (Sigma-Aldrich H4908). Alexa-conjugated secondary antibodies (Alexa555-donkey anti
391 rabbit, Alexa488-donkey anti rabbit, Alexa488-donkey anti mouse) were used at 1:1000 dilution.
392 1 g/ml DAPI was added at the end to stain nuclei. Images were acquired with Zeiss Axio
393 fluorescence microscopy.

394 **Quantitative RT PCR**

395 mRNA were extracted with the NucleoSpin RNA kit (Machery-Nagel) according to manufacturer's
396 instructions. cDNA were generated with the iScript cDNA Synthesis kit (BIO-RAD) according to
397 the manufacturer's instructions. Real-time quantitative RT-PCR was performed using a
398 LightCycler 480 (Roche Applied Science).

399 **Western Blot**

400 Cells were lysed in SDS buffer (2% SDS, 150mM NaCl, 50mM Tris-HCl, pH 7.4), denaturated at
401 94℃ for 5 minutes. Protein concentration was measured with the BCA assay kit using BSA as a
402 standard (Pierce Biotechnology, Rockford, IL, USA) according to manufacturer's instructions. The
403 primary antibodies used were : anti-HA (1:1000 dilution, Sigma-Aldrich H4908), anti-LC3 (1:1000
404 dilution, Cell signaling) and an anti-actin conjugated with HRP ().

405 **Proximity-Dependent Biotinylation assay**
406
407 In order to identify new partners of the K1 induced signalization, a proximity biotinylation
408 screening of the receptor K1 was performed. The receptor K1 was fused to the soybean ascorbate
409 peroxydase (APEX2) in a Tet–ON/OFF plasmid (PITR). MDA-MB 231 cell line was stably
410 transfected with the PITR K1-APEX2 plasmid expressing the receptor fused to APEX under DOX
411 treatment. For each biotinylation experiment 30 million cells were seeded. 2 conditions were
412 chosen, a control condition without induction of K1 (DOX 0) and the dox treated condition (DOX
413 0.25). DOX (0.25 µg/mL) was added 24 hours after seeding and biotinylation was performed after
414 24 hours of treatment. 500 µm Biotin Phenol (BP) in DMEM and incubated for 30 minutes at 37°C.
415 Fresh diluted H_2O_2 was then directly added in BP/DMEM at a concentration of 1 mM for 1 minute.
416 After 1 minute, the supernatant was collected and 15 mL of a quenching solution (10 mM sodium
417 ascorbate – 5 mM Trolox – 10 mM sodium azide solution) was added to the dish to stop the
418 biotinylation reaction.
419

420 Three washing steps were repeated in 20 mL quenching solution. Between each washing step, cells
421 were centrifugated for 4 minutes. The quenching solution was then discarded. A centrifugation for
422 10 minutes was then performed. The quenching solution was aspirated and the dry pellet was lysed.
423 RIPA lysis buffer supplemented with 1X protease inhibitor cocktail and with quencher at 1X was
424 used. RIPA lysis buffer was made in a total volume of 50 mL, containing: 12.5 mL Tris Hcl (250
425 mM), 7.5 mL NaCl (750 mM), 1.25 mL SDS 20% (0.5% final), 12.5 mL NaDeoxy 10% (2.5%
426 final),2.5 mL NP40 (5% final) and 13.75 mL H2O. For each condition, 500µL of lysis buffer was
427 used. Samples were vortexed to facilitate lysis. Protein concentration was measured with
428 Pierce 660nm protein assay kit (ThermoFicher scientific). 2 mg of proteins was used for enrichment
429 on 100µL of streptavidin magnetic beads (ROCHE, ref 11641786001) at +4°C for 2 hours. The
430 supernatant was then discarded and beads washed at 4°C for 5 minutes twice with RIPA buffer,
431 once with KCl (1M), once with Na_2CO_3 (0.1M) and twice Urea (2M) in Tris HCl 10 mM at pH 8.0.
432
433 Proteins were then eluted for 10 minutes at 95°C in a protein loading buffer supplemented with
434 biotin (2 mM) and DTT (20 mM). Samples were then quickly vortexed and cooled on ice for 5-10
435 minutes. Beads were then pelleted using a magnetic rack, frozen at -80°C and sent to the mass
436 spectrometry (MS) platform EDyP in Grenoble on dry ice.
437

438 **Statistical analysis**

439 If samples followed a Gaussian distribution, one-way ANOVA or two-way ANOVA were applied,
440 either paired-ratio or unpaired depending on the experimental data. When samples did not pass the
441 normality test, non-parametric test was applied (Mann-Whitney for unpaired samples and
442 Wilcoxon signed-rank test for paired samples). * : $p<0,05$; ** : $p<0,01$; *** : $p<0,001$.

443

444

445 **REFERENCES**

446 1. Negulescu A, Mehlen P. Dependence receptors – the dark side awakens. FEBS J 2018;
447 285:3909–24.

448 2. Ichim G, Genevois A-L, Ménard M, Yu L-Y, Coelho-Aguiar JM, Llambi F, Jarrosson-Wuilleme
449 L, Lefebvre J, Tulasne D, Dupin E, et al. The Dependence Receptor TrkC Triggers
450 Mitochondria-Dependent Apoptosis upon Cobra-1 Recruitment. Molecular Cell 2013;
451 51:632–46.

452 3. Wang H, Boussouar A, Mazelin L, Tauszig-Delamasure S, Sun Y, Goldschneider D, Paradisi
453 A, Mehlen P. The Proto-oncogene c-Kit Inhibits Tumor Growth by Behaving as a Dependence
454 Receptor. Molecular Cell 2018; 72:413-425.e5.

455 4. Fombonne J, Bissey P-A, Guix C, Sadoul R, Thibert C, Mehlen P. Patched dependence receptor
456 triggers apoptosis through ubiquitination of caspase-9. Proc Natl Acad Sci USA 2012;
457 109:10510–5.

458 5. Causeret F, Sumia I, Pierani A. Kremen1 and Dickkopf1 control cell survival in a Wnt-
459 independent manner. Cell death and differentiation 2016; 23:323–32.

460 6. Mao B, Wu W, Davidson G, Marhold J, Li M, Mechler BM, Delius H, Hoppe D, Stannek P,
461 Walter C, et al. Kremen proteins are Dickkopf receptors that regulate Wnt/beta-catenin
462 signalling. Nature 2002; 417:664–7.

463 7. Wang K, Zhang Y, Li X, Chen L, Wang H, Wu J, Zheng J, Wu D. Characterization of the
464 Kremen-binding site on Dkk1 and elucidation of the role of Kremen in Dkk-mediated Wnt
465 antagonism. The Journal of biological chemistry 2008; 283:23371–5.

466 8. Mishra SK, Funair L, Cressley A, Gittes GK, Burns RC. High-affinity Dkk1 receptor Kremen1
467 is internalized by clathrin-mediated endocytosis. PloS one 2012; 7:e52190.

468 9. Yamamoto H, Sakane H, Yamamoto H, Michiue T, Kikuchi A. Wnt3a and Dkk1 regulate
469 distinct internalization pathways of LRP6 to tune the activation of beta-catenin signaling.
470 Developmental cell 2008; 15:37–48.

471 10. Davidson G, Mao B, del Barco Barrantes I, Niehrs C. Kremen proteins interact with Dickkopf1
472 to regulate anteroposterior CNS patterning. Development 2002; 129:5587–96.

473 11. Mukhopadhyay M, Shtrom S, Rodriguez-Esteban C, Chen L, Tsukui T, Gomer L, Dorward
474 DW, Glinka A, Grinberg A, Huang SP, et al. Dickkopf1 is required for embryonic head
475 induction and limb morphogenesis in the mouse. Developmental cell 2001; 1:423–34.

476 12. Staring J, Van Den Hengel LG, Raaben M, Blomen VA, Carette JE, Brummelkamp TR.
477 KREMEN1 Is a Host Entry Receptor for a Major Group of Enteroviruses. Cell Host &
478 Microbe 2018; 23:636-643.e5.

479 13. Nakamura T, Nakamura T, Matsumoto K. The functions and possible significance of Kremen

480 as the gatekeeper of Wnt signalling in development and pathology. Journal of cellular and
481 molecular medicine 2008; 12:391–408.

482 14. Sato N, Yamabuki T, Takano A, Koinuma J, Aragaki M, Masuda K, Ishikawa N, Kohno N, Ito
483 H, Miyamoto M, et al. Wnt inhibitor Dickkopf-1 as a target for passive cancer
484 immunotherapy. Cancer research 2010; 70:5326–36.

485 15. Rachner TD, Thiele S, Gobel A, Browne A, Fuessel S, Erdmann K, Wirth MP, Frohner M,
486 Todenhofer T, Muders MH, et al. High serum levels of Dickkopf-1 are associated with a poor
487 prognosis in prostate cancer patients. BMC cancer 2014; 14:649.

488 16. Sun DK, Wang L, Wang JM, Zhang P. Serum Dickkopf-1 levels as a clinical and prognostic
489 factor in patients with bladder cancer. Genetics and molecular research : GMR 2015;
490 14:18181–7.

491 17. Zhou SJ, Zhuo SR, Yang XQ, Qin CX, Wang ZL. Serum Dickkopf-1 expression level positively
492 correlates with a poor prognosis in breast cancer. Diagnostic pathology 2014; 9:161.

493 18. Huang Y, Yang X, Zhao F, Shen Q, Wang Z, Lv X, Hu B, Yu B, Fan J, Qin W. Overexpression
494 of Dickkopf-1 predicts poor prognosis for patients with hepatocellular carcinoma after
495 orthotopic liver transplantation by promoting cancer metastasis and recurrence. Medical
496 oncology 2014; 31:966.

497 19. Cui Y, Parashar S, Zahoor M, Needham PG, Mari M, Zhu M, Chen S, Ho H-C, Reggiori F,
498 Farhan H, et al. A COPII subunit acts with an autophagy receptor to target endoplasmic
499 reticulum for degradation. Science 2019; 365:53–60.

500 20. Li Z, Huang W, Wang W. Multifaceted roles of COPII subunits in autophagy. Biochimica et
501 Biophysica Acta (BBA) - Molecular Cell Research 2020; 1867:118627.

502 21. Gui X, Yang H, Li T, Tan X, Shi P, Li M, Du F, Chen ZJ. Autophagy induction via STING
503 trafficking is a primordial function of the cGAS pathway. Nature 2019; 567:262–6.

504 22. Xun J, Zhang Z, Lv B, Lu D, Yang H, Shang G, Tan JX. A conserved ion channel function of
505 STING mediates noncanonical autophagy and cell death. EMBO Rep 2024; 25:544–69.

506 23. Holzer E, Martens S, Tulli S. The Role of ATG9 Vesicles in Autophagosome Biogenesis.
507 Journal of Molecular Biology 2024; 436:168489.

508 24. Matoba K, Kotani T, Tsutsumi A, Tsuji T, Mori T, Noshiro D, Sugita Y, Nomura N, Iwata S,
509 Ohsumi Y, et al. Atg9 is a lipid scramblase that mediates autophagosomal membrane
510 expansion. Nat Struct Mol Biol 2020; 27:1185–93.

511 25. Davis S, Wang J, Zhu M, Stahmer K, Lakshminarayan R, Ghassemian M, Jiang Y, Miller EA,
512 Ferro-Novick S. Sec24 phosphorylation regulates autophagosome abundance during nutrient
513 deprivation. eLife 2016; 5:e21167.

514 26. Brisset M, Grandin M, Bernet A, Mehlen P, Hollande F. Dependence receptors: new targets for

515 cancer therapy. EMBO Mol Med 2021; 13:e14495.

516 27. Berthenet K, Diazzi S, Jamard C, Stopa K, Dragan S, Fanfone D, Nguyen T, Al N, Virard F,
517 Meurette O, et al. Atypical contribution of caspase-3 to melanoma cancer cell motility by
518 regulation of coronin 1B activity [Internet]. 2024 [cited 2024 Oct 31]; Available from:
519 http://biorxiv.org/lookup/doi/10.1101/2024.06.27.601010

520 28. Schweichel JU, Merker HJ. The morphology of various types of cell death in prenatal tissues.
521 Teratology 1973; 7:253–66.

522 29. Marino G, Niso-Santano M, Baehrecke EH, Kroemer G. Self-consumption: the interplay of
523 autophagy and apoptosis. Nature reviews Molecular cell biology 2014; 15:81–94.

524 30. Huang Z, Zhou L, Chen Z, Nice EC, Huang C. Stress management by autophagy: Implications
525 for chemoresistance. International journal of cancer 2016; 139:23–32.

526 31. Denton D, Shravage B, Simin R, Mills K, Berry DL, Baehrecke EH, Kumar S. Autophagy, not
527 apoptosis, is essential for midgut cell death in Drosophila. Current biology : CB 2009;
528 19:1741–6.

529 32. Berry DL, Baehrecke EH. Growth arrest and autophagy are required for salivary gland cell
530 degradation in Drosophila. Cell 2007; 131:1137–48.

531 33. Liu Y, Shoji-Kawata S, Sumpter RM, Wei Y, Ginet V, Zhang L, Posner B, Tran KA, Green DR,
532 Xavier RJ, et al. Autosis is a Na+,K+-ATPase–regulated form of cell death triggered by
533 autophagy-inducing peptides, starvation, and hypoxia–ischemia. Proc Natl Acad Sci U S A
534 2013; 110:20364–71.

535 34. Button RW, Roberts SL, Willis TL, Hanemann CO, Luo S. Accumulation of autophagosomes
536 confers cytotoxicity. J Biol Chem 2017; 292:13599–614.

537 35. Kriel J, Loos B. The good, the bad and the autophagosome: exploring unanswered questions
538 of autophagy-dependent cell death. Cell Death Differ 2019; 26:640–52.

539 36. Wu M, Zhang X, Zhang W, Chiou YS, Qian W, Liu X, Zhang M, Yan H, Li S, Li T, et al. Cancer
540 stem cell regulated phenotypic plasticity protects metastasized cancer cells from ferroptosis.
541 Nat Commun 2022; 13:1371.

542 37. Nassour J, Radford R, Correia A, Fusté JM, Schoell B, Jauch A, Shaw RJ, Karlseder J.
543 Autophagic cell death restricts chromosomal instability during replicative crisis. Nature 2019;
544 565:659–63.

545 38. Nassour J, Aguiar LG, Correia A, Schmidt TT, Mainz L, Przetocka S, Haggblom C, Tadepalle
546 N, Williams A, Shokhirev MN, et al. Telomere-to-mitochondria signalling by ZBP1 mediates
547 replicative crisis. Nature 2023; 614:767–73.

548

549

550 **Figure legends**

551 **Figure 1: The Kremen-1/DKK1 pair is altered in cancers.**

552 (**A,B**) Kremen1 (A) and DKK1 (B) expression was assessed in paired Normal /Tumoral sample
553 from different cancers from TCGA dataset. (**C,D**) Kaplan-Meier survival analysis of DKK1
554 expression (low or high) in pancreatic adenocarcinoma (**C**) and breast cancer (**D**) patients from the
555 TCGA dataset. (**E-H**) Violin plot of DKK1 (**E,F**) and Kremen1 (**G,H**) expression across different
556 subtypes of breast cancer patients from the TCGA dataset (**E,G**) and metabric (**F,H**).

557

558 **Figure 2: Kremen1 does not induce apoptotic cell death**

559 (**A**) Cell death was measured by propidium iodide incorporation in MDA-MB-231 with or without
560 Kremen1 expression upon doxycycline treatment (0,5 and 2 µg/mL). (**B**) Colony formation assay
561 using crystal violet with or without Kremen1 expression following dox treatment (dox 2µg/mL)
562 and quantification of the colonies. (**C**) Cell death measured by propidium iodide incorporation
563 upon Kremen1 expression +/- DKK1 expression and western blot analysis showing the expression
564 of Kremen1 in the different cell lines. (**D**) Caspase-3 activity was measured in presence or not of
565 Kremen1 expression (dox) and q-VD-oph treatment (5µM). (**E**) Cell death was measured by
566 propidium iodide incorporation +/- Kremen1 expression and qVD-oph treatment (5µM). (**F**)
567 Nanolive imaging analysis comparing Kremen1 expressing cells and apoptotic cells treated with
568 BV6 (1µM).

569

570 **Figure 3: Kremen1 induced-cell death displays autophagic features**

571 (**A**) Electronic transmission microscopy of MD-AMB-231 cells expressing Kremen1 showing
572 numerous vacuoles. (**B**) Western blot showing LC3 and p62 expression upon doxycycline
573 treatment at 8h, 14h and 24 hours. (**C**) Immunofluorescence staining using LC3 antibody, DAPI in
574 control cells or Kremen1 expressing cells. (**D**) Immunofluorescence staining and confocal
575 microscopy using LC3B antibody and DAPI on BxPC3 cells. (**E**) Western blot showing LC3 and
576 p62 expression upon doxycycline treatment in MDA-MB-231 cell line expressing Kremen1 or
577 Kremen1 and DKK1.

578

579

580 **Figure 4: Kremen1-induced cell death is dependent on ATG9A**

581 (**A**) Measure of cell death by propidium iodide incorporation following Kremen1 expression
582 (DOX) +/- spautin (1μM) (**A**) or +/- Wortmannin (**B**) and western blot analysis of autophagic
583 markers following Kremen1 expression and spautin (1μM, **A**) or wortmannin (1, 2,5 and 5 μM, **B**).
584 (**C,D**) Measure of cell death following kremen1 induction (Dox 0.25 or 2 μg/ml) +/- Bafilomycin
585 A1 (**C**) or Chloroquine treatment (**D**). (**E**) Confocal analysis of immunofluorescence staining with
586 ATG9A and Kremen1 antibodies in BxPC3 cells following Kremen1 induction. (**F,G**) Monitoring
587 of cell death following anti-ATG9A (**F**) or anti-ATG18B (**G**) siRNA transfection of MDA-MB-
588 231 cells following Kremen1 induction.
589
590
591 **Figure 5: SEC24C is implicated in Kremen1-induced cell death**
592 (**A**) Volcano plot showing protein identified by mass spectrometry in Kremen1 interactome. (**B**)
593 STRING database protein interaction network map highlighting members of the COP-II complex
594 revealed by mass spectrometry. (**C**) Protein Ligation Assay (PLA) performed on cells with only
595 Kremen1 antibody or Kremen1 and Sec24C antibodies in MDA-MB-231 cells. (**D**) Confocal
596 imaging showing cells stained with DAPI, Kremen1 antibody (red) or Sec24C antibody (Green)
597 and merged on BxPC3 cell line treated with DOX. (**E**) Cell death induction following Kremen1
598 induction (dox, 2μg/ml) and knock-down of SEC24C by siRNA in MDA-MB -and BxPC3 cells.
599
600 **Figure 6: Kremen1 induced SEC24C interaction with ATG8**
601 (**A**) Monitoring of autophagic marker LC3 following inhibition of Sec24C by siRNA at 12h, 14h
602 and 36h and associated quantification at 24h. (**B**) Western blot analysis following
603 immunoprecipitation of Sec24C upon Kremen1 expression and associated quantification. (**C**)
604 Confocal imaging showing cells stained with LC3 (red) Sec24C (Green) or DAPI following
605 Kremen1 induction. (**D**) PLA images and quantification of ATG9/K1 interaction in presence of
606 Kremen1 induction with or without DKK1 induction and associated quantification.
607

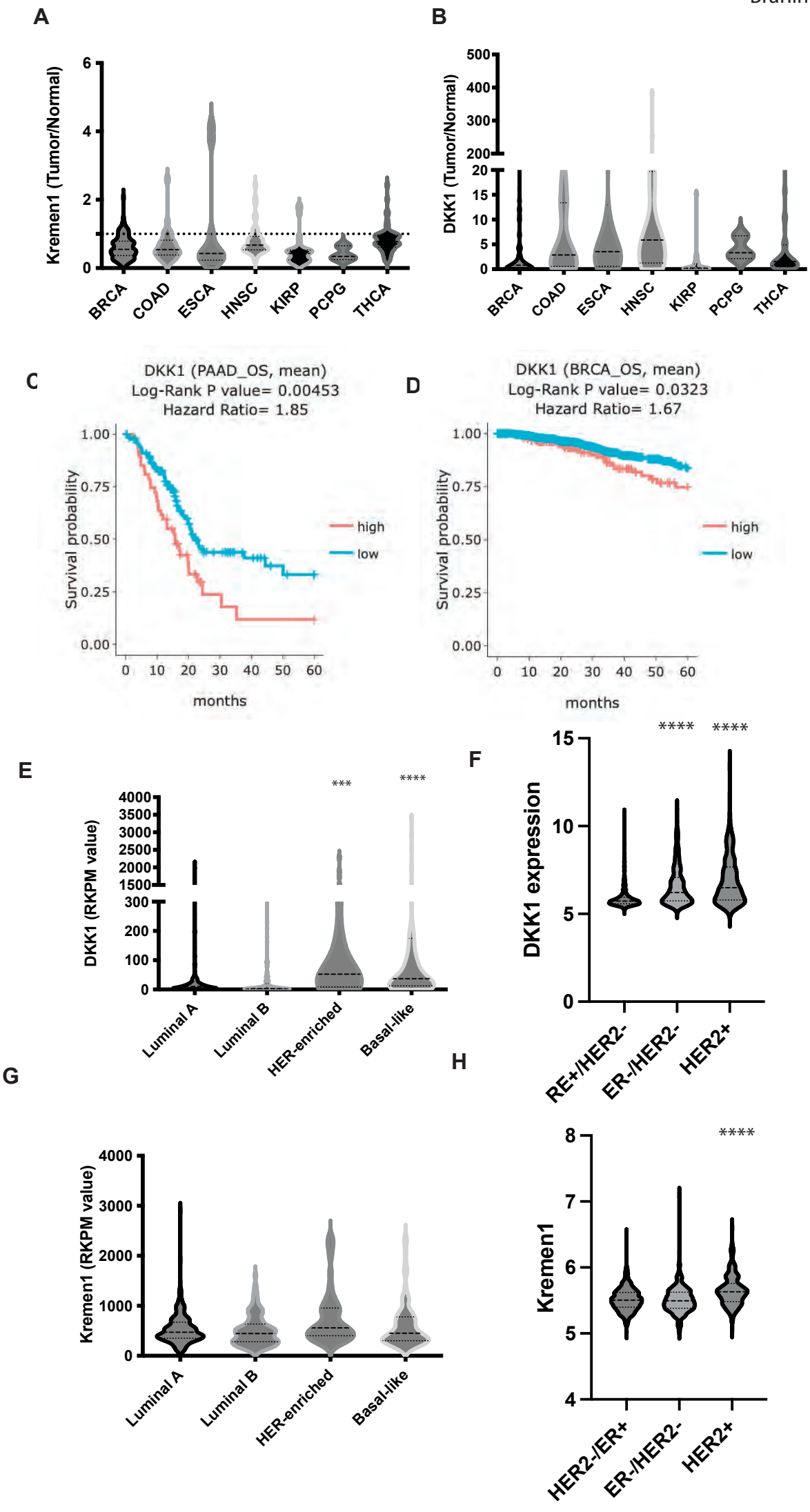
A
Kremen1 (Tumor/Normal)
BRCA
COAD
ESCA
HNSC
KIRP
PCPG
THCA
B
DKK1 (Tumor/Normal)
C
DKK1 (PAAD_OS, mean)
Log-Rank P value= 0.00453
Hazard Ratio= 1.85
Survival probability
months
high
low
D
DKK1 (BRCA_OS, mean)
Log-Rank P value= 0.0323
Hazard Ratio= 1.67
E
DKK1 (RKPM value)
Luminal A
Luminal B
HER-enriched
Basal-like
F
DKK1 expression
RE+/HER2-
ER-/HER2-
HER2+
G
Kremen1 (RKPM value)
H
Kremen1
HER2-/ER+

Brahim, Schott et al., Figure 2

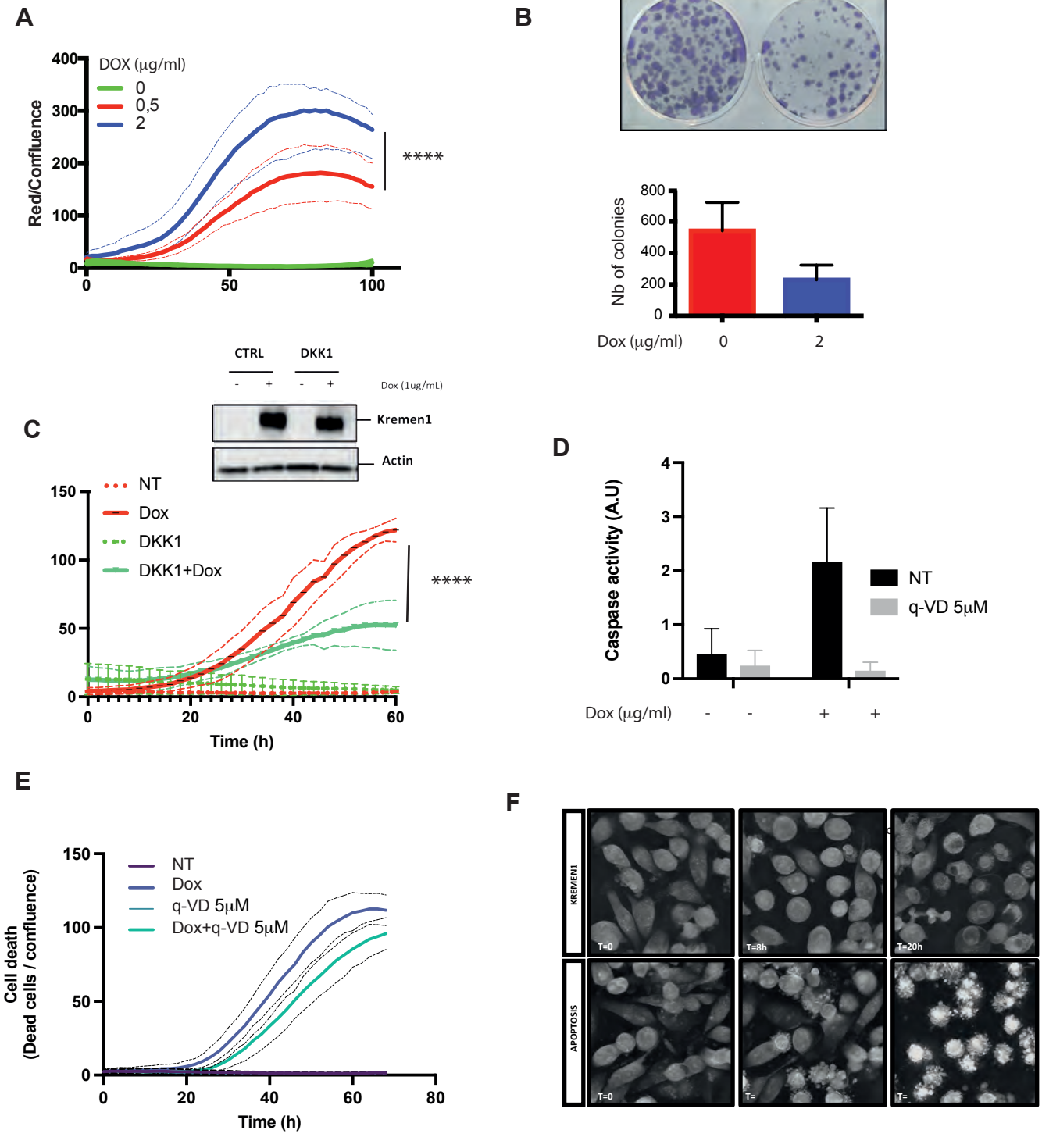

Brahim, Schott et al., Figure 3

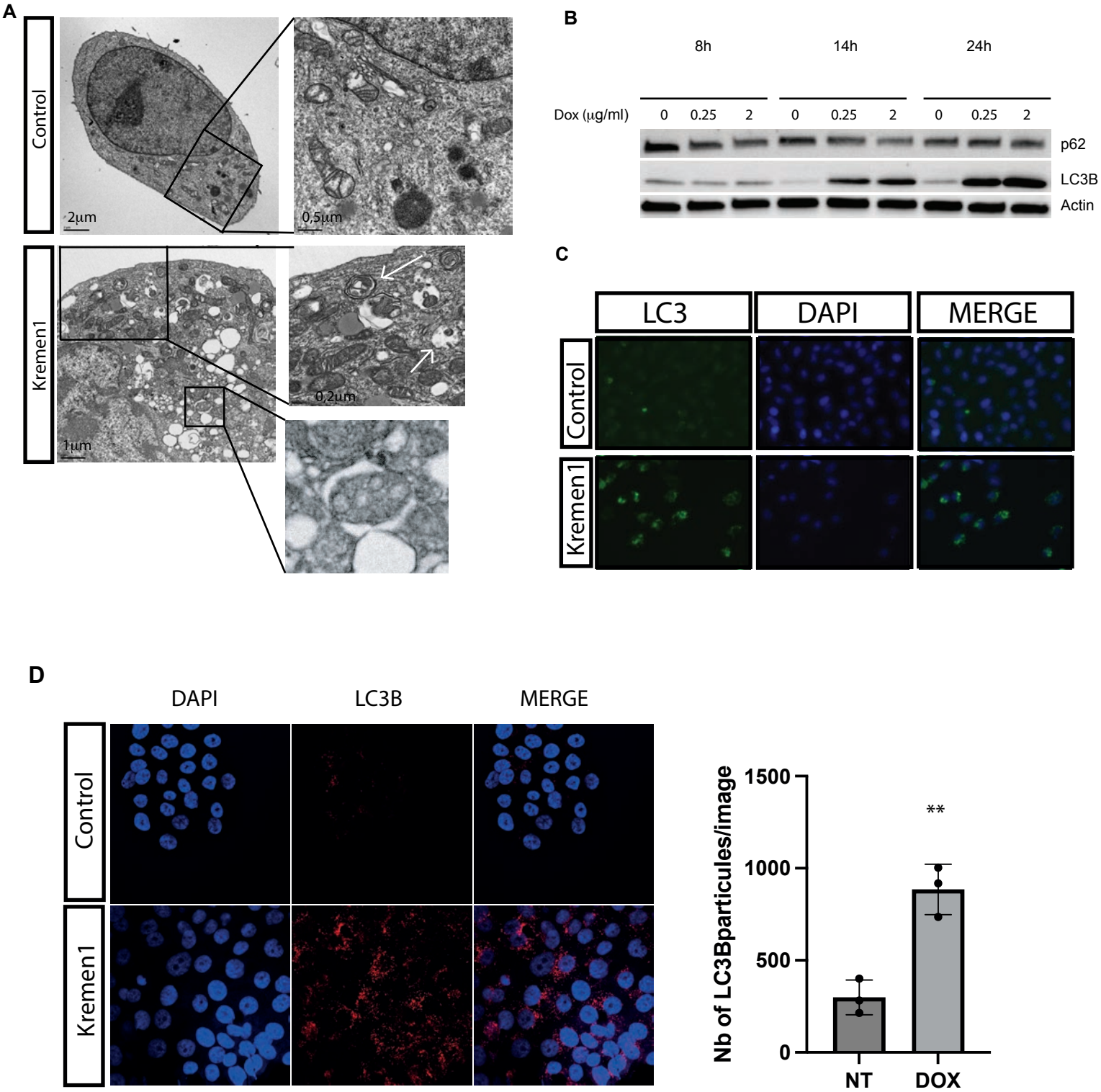

Brahim, Schott et al., Figure 4

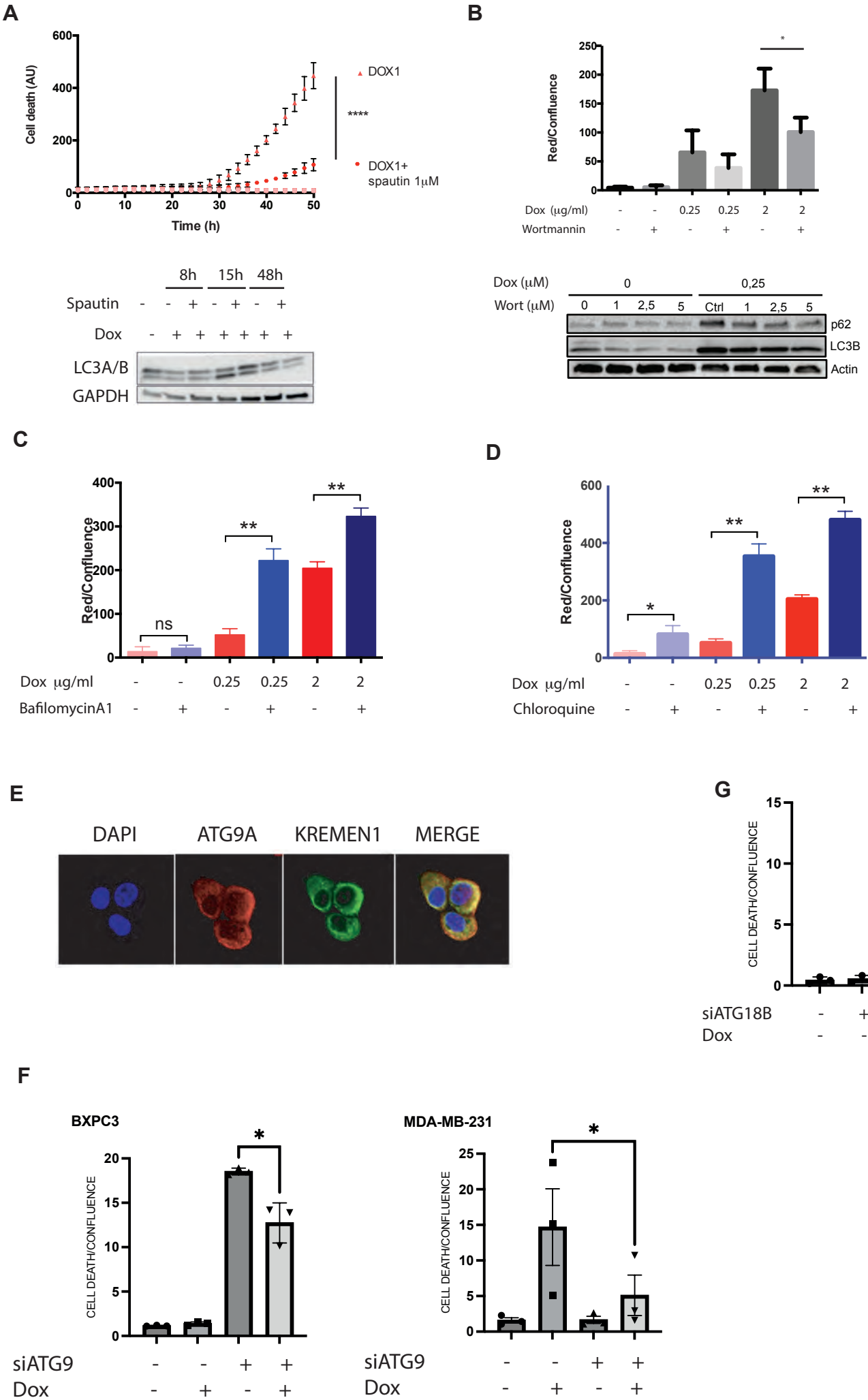

Brahim, Schott et al., Figure 5

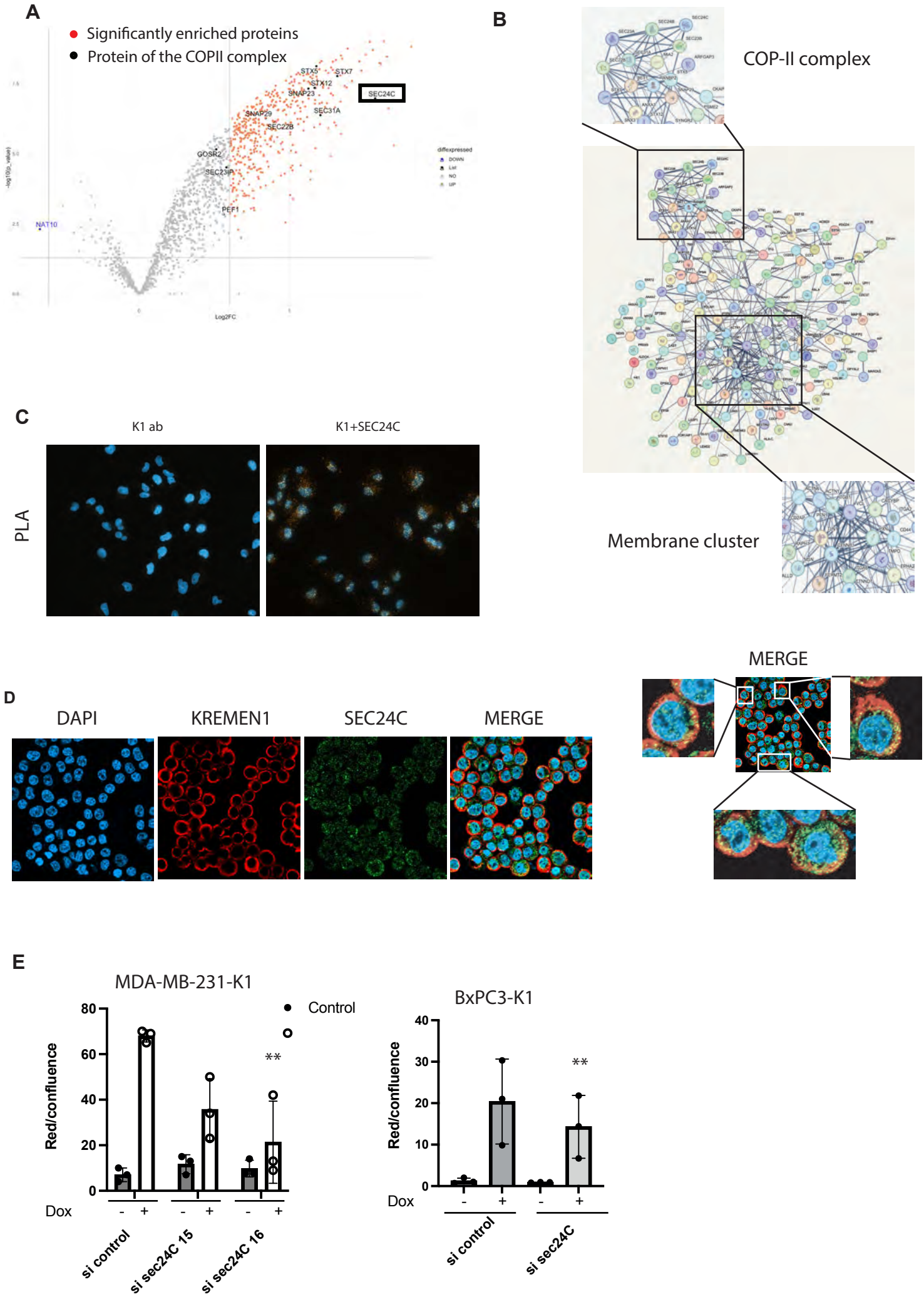
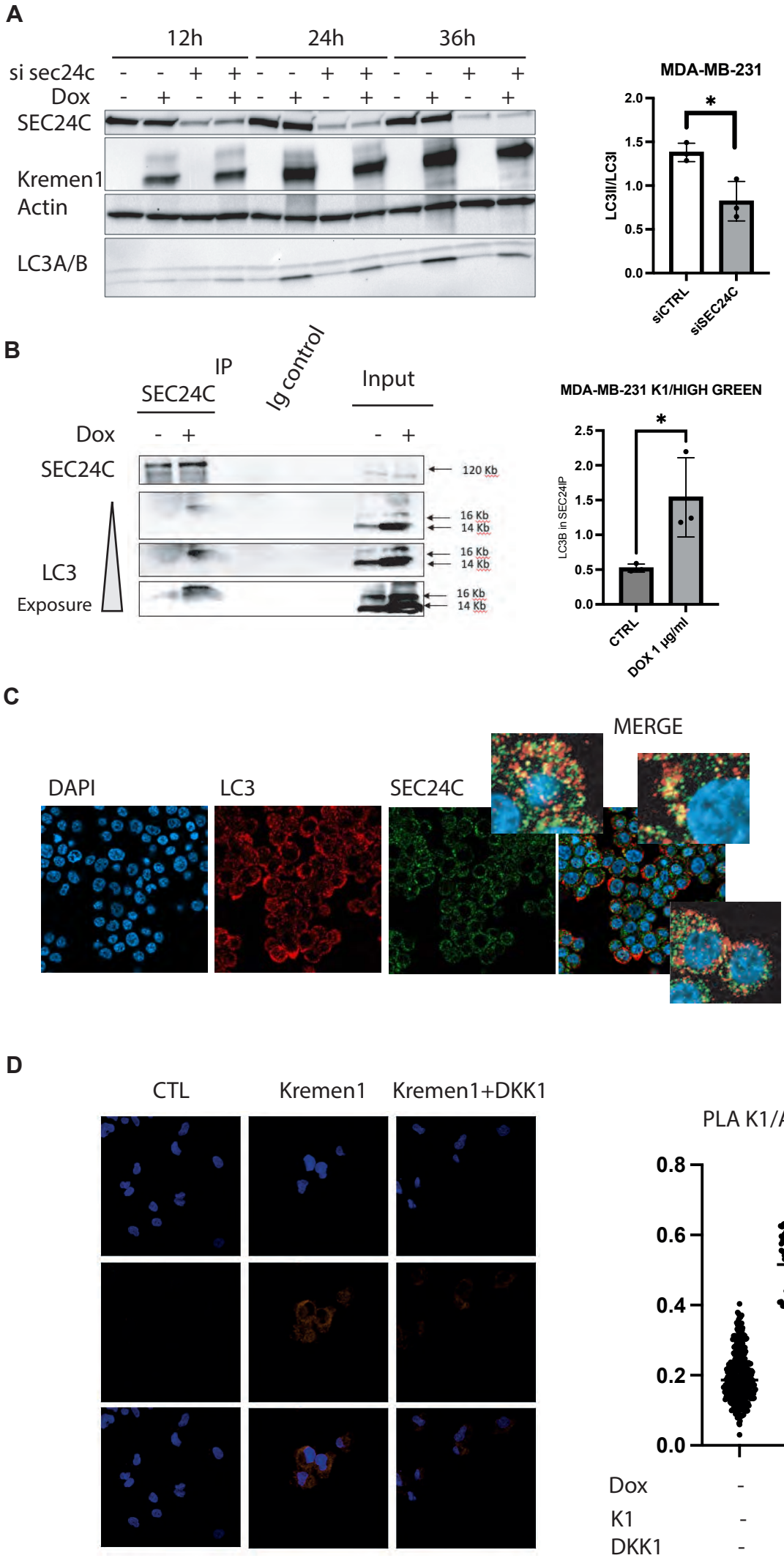
Brahim, Schott et al., Figure 6